Quantifying effects of upper motor neuron degeneration on the wrist in amyotrophic lateral sclerosis

By

J. J. Plouvier

in partial fulfilment of the requirements for the degree of

Master of Science
in Biomedical Engineering

at the Delft University of Technology,
to be defended publicly on Friday, September 30, 2022 at 09:30 AM.

Thesis committee:	Prof. dr. F.C.T. van der Helm	TU Delft
	Dr. Ir. B.T.H.M Sleutjes	UMC Utrecht
	Ir. D.J.L Stikvoort	UMC Utrecht

TU Delft

Contents

Abstract

Background: Amyotrophic lateral sclerosis (ALS) is a motor neuron disease that is characterized by the degeneration of upper and lower motor neuron (UMN, LMN). A defining feature of ALS is its heterogeneous presentation, with varying sites of disease onset and progression rate. Diagnosing ALS requires the observation of both UMN and LMN degeneration in multiple regions of the body. Signs of UMN degeneration are difficult to observe in ALS. The goal of this study was to determine if reflexive parameters were related to UMN dysfunction in ALS patients.

Methods: A robot applied continuous torque perturbations to the right wrist of the subjects. Subject were asked to perform 4 different tasks, each provoking different control strategies. Closed-loop system identification was used to estimate the joint dynamics. A neuromuscular model was then fitted to the estimated joint dynamics to express the contribution of intrinsic and reflexive pathways in physiologically relevant parameters.

Results: We show that patients are able to alter their joint dynamics in order to comply with the tasks. During the relax task patients had visibly higher admittance than controls, in the active tasks the patients were able to lower their admittance similar as controls. Patients with pathologically increased reflexes had significantly increased reflexive feedback during the force tasks compared to controls.

Conclusion: In this study we have demonstrated the ability of neuromechanical parameters to detect hyperreflexia in patients diagnosed in ALS. Therefore the proposed method of closed-loop system identification and parameters estimation could be used to monitor the progression of ALS.

1 Introduction

1.1 Background

Amyotrophic lateral sclerosis (ALS) is a progressive motor neuron disease which is characterized by upper and lower motor neuron (UMN, LMN) loss, that spreads to multiple regions over time[1]. The disease is markedly heterogeneous, with varying sites of disease onset and progression rate. Therefore, identifying reliable biomarkers for the disease and its progression remains a high priority, especially for UMN loss[2]. Diagnosis of ALS requires evidence of both UMN and LMN degeneration in different regions of the body[3]. Classical evidence of UMN loss includes: weakness, increased tendon reflexes and spasticity[4]. LMN degeneration is characterized by: weakness, muscle wasting, fasciculations, reduced muscle tone and absent or reduced tendon reflexes. In addition, proprioceptive information is integrated and modulated at the spinal cord by UMNs, and subsequently expressed over the LMNs[28] (figure 1A). The loss of LMNs causes the pathway where the UMN symptoms are expressed to be disrupted, making the symptoms difficult to elicit[5]. This complex interplay between UMN and LMN symptoms makes it increasingly difficult to observe classical symptoms of the UMN syndrome[5]. The interaction between the UMN and LMN can be described by a closed-loop. Signals from the UMN are send to the LMN which in turn sends a signal to the muscle, proprioceptors in the muscle provide feedback of the position and force on the muscle to the UMN in the central nervous system (figure 1B). Quantitative examination of neuromuscular properties in ALS may, therefore, benefit from the application of closed-loop identification techniques.

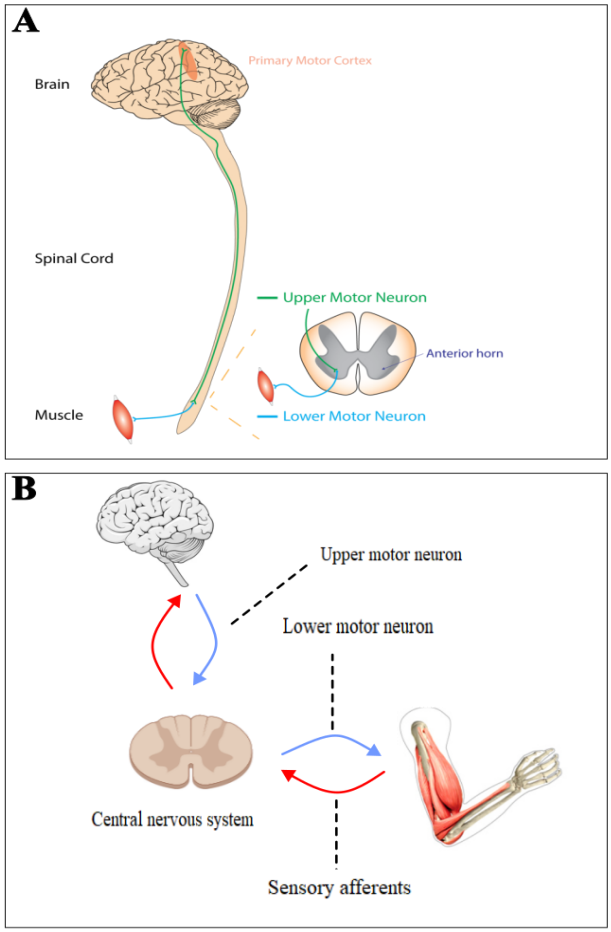

Figure 1 A) Physiologic representation of the interaction of the UMN with the LMN. A signal from the UMN travels from the motor cortex via the corticospinal tract to the LMN, where the signal is carried from the spinal column to the muscle. B) Representation of the closed-loop between the UMN, LMN and sensory afferents.

In studies of human motor control closed-loop identification techniques are used[6-10]. Herein, the UMNs of the central nervous system (CNS) act as the controller, proprioceptive organs act as sensors providing feedback to the controller and muscles function as actuators. System identification (SI) techniques can then be used to capture the dynamics of the limb. In human motor control the dynamics of a limb are studied by perturbing the limb with a robot. Modelling the relationship between the torque input and the displacement of the limb the dynamics of the limb can be estimated. In order to accurately describe the dynamics of the system, it is important that the input is precise and well-known[7].

Two effective pathways can be employed to control the limb during perturbations. The first pathway relies on direct activation of the muscles, resulting in contraction and altered muscle viscoelasticity. This voluntary modulation of muscle viscoelasticity is defined as the intrinsic pathway in the human motor control model. The second mechanism relies on integration of proprioceptive information. Muscle spindles (MS) provide information on the muscle stretch and the velocity of the stretch and the Golgi tendon organs (GTO) provide information on the active muscle strength. This proprioceptive modulation of muscle activity is defined as the reflexive pathway in the model. Hence, contributions of the reflexive pathway are expressed in a feedback loop, and contributions of the intrinsic pathway originate directly from supraspinal regions. Of note, in activities of daily life (ADL) both pathways work in tandem and leverage each other's strengths to achieve optimal performance and control[8]. The properties of the intrinsic and reflexive pathways are then captured by physiologically relevant parameters by fitting a neuromuscular model (NMM) to the identified dynamics[11].

This method of SI and parameter estimation with a NMM has been implemented in various studies of UMN diseases. In stroke and cerebral palsy tissue stiffness and viscosity and reflexive parameters were found to be correlated to Ashworth scores of rigidity and spasticity [12-14]. In Parkinson's disease rigidity was separated into contributions from reflexive behavior and intrinsic mechanical resistance, where the contribution from the neural reflexes were greater than the intrinsic contributions[15,16]. The effect of dopaminergic medication was found to be greater on the neural reflexes, which was expected[16]. These studies were able to find significant differences in patients compared to controls and most studies were able to separate patients based on clinical scores. Therefore, this method has the potential to be a useful measure of disease progression and effects of medication. As studies in the field of UMN diseases show SI and parameter estimation can be used to measure the effects of UMN lesions on intrinsic and reflexive properties of a limb[12-16]. Currently studies of UMN degeneration in ALS use diffusion tensor MRI and transcranial magnetic stimulation (TMS). Diffusion tensor MRI evaluates the UMN fiber tract integrity[33-34] and TMS evaluates the integrity of the UMN tracts[35]. These methods provide structural information about the degeneration of the UMN but are not able to assess the effect on functioning. Clinical examination remains the best way to localize and monitor

neurodegeneration in vivo[36]. Applying continuous perturbations to a limb when performing a task enables the dynamics of the limb to be studied during functional movements. Making it possible to estimate the contributions of UMN degeneration to functional behavior. Yet, these techniques remain unexplored in ALS. In this study closed-loop SI techniques were used to explore if UMN degeneration in ALS patients is reflected by estimated neuromechanical parameters. We measured the arm in both active and relaxed states, to assess the effects of ALS in active states. We hypothesize that reflexive parameters, pertaining to the integration of feedback from the type Ia and II afferents in the MS and the type Ib afferent from the GTO, are closely related with clinical examinations in the relaxed state.

1.2 Problem statement

Diagnosis and monitoring of ALS is reliant on the observation of clinical signs of UMN degeneration. Due to the degeneration of the LMNs, signs of UMN dysfunction are difficult to elicit in ALS[30].

1.3 Objective

The object of this study is to explore if neuromechanical parameters are a sensitive tool to quantify degeneration of UMNs in ALS. And ultimately be a quantitative measure of UMN degeneration in ALS and assisting in the monitoring of disease progression in ALS.

1.4 Approach

This study uses closed-loop SI and parameter estimation to express the dynamics of the wrist in physiologically relevant neuromechanical parameters. Closed loop SI requires the use of perturbations that are well-known and precise[32]. Perturbations are applied to the right wrist by a robot manipulator. Torque on and position of the handle are measured and together with recorded EMG are used to estimate the dynamics of the wrist.

2 Methods

2.1 Participants

In this cross-sectional cohort study we recruited 15 patients diagnosed with ALS from the clinic of the University Medical center Utrecht between (sept. 2021-jul. 2022). Exclusion criteria included the presence of active psychiatric disorders such as frontotemporal dementia, a history or presence of brain injury, epilepsy, and other cerebral pathologies. Further exclusion criteria were: concomitant polyneuropathies or isolated neuropathies in the arm (e.g. carpal tunnel syndrome) and a Medical Research Council (MRC) score of 2 or less in the flexor or extensor carpi radialis (FCR, ECR). The MRC scale is a measure of muscle strength with the following scores: 0, paralysis; 1, only a trace of muscle contraction is seen; 2, muscle movement is possible without gravity; 3, muscle movement is possible against gravity; 4, reduced muscle strength but movement against resistance is possible; 5, normal muscle strength[31]. A set of reference neuromuscular parameters was derived from 15 healthy participants. All patients and controls gave informed consent. The study was performed in accordance with the Declaration of Helsinki and was approved by the medical ethics committee of the University Medical Centre Utrecht.

2.2 Procedure

Participants were seated in a chair with their elbow flexed approximately 1m from a computer screen. The arm was cleaned and two sets of bipolar surface electrodes (Red Dot, 3M Health Care, Neuss, Germany) were placed on the muscle belly of the FCR and ECR muscles. Muscle activation was recorded using a TMSi REFA amplifier (TMSi, Oldenzaal, the Netherlands). A Wristalyzer single-axis wrist manipulator (Moog FCS, Nieuw Vennep, the Netherlands)[17] was used to apply unpredictable multisine torque perturbations[18] and measure the resulting wrist rotations and torques. The hand was fixated on the handle with Velcro straps and the arm was placed in an arm rest to isolate wrist motion. We aligned the motor axis of the robot with the rotational axis of the wrist joint. The screen in front of the participant was used for task instruction and visual indication of the handle position.

2.3 Clinical assessment

Clinical assessment of the ALS patients was performed by an experienced physician. This examination contained a neurological examination and clinical rating of disease progression. Progression of ALS was measured by the Revised ALS Functional Rating Scale (ALSFRS-R)[27]. The ALSFRS-R is a questionnaire that tracks and measures progression of disability in 12 items across bulbar, gross motor tasks, fine motor tasks and respiratory function. These 12 items are scored 0-4 so the maximum score is 48. Fine motor function (FMF) is measured by the items 4, 5 and 6. For the purpose of this study item 6 was excluded. From the neurological examination the reflexes and muscle tone of the right arm were obtained. We categorized the reflexes by the following measures: normal, elevated and pathological reflex activity. Reflexes of FCR and ECR muscles are not tested directly. The FCR and ECR are innervated by the median and radial nerve respectively, which both originate from cervical nerve roots C6 and C7. Reflex arcs from these nerve roots are assessed by the biceps (C5,C6) and triceps (C7,C8) reflex. Therefore, the reflex activity captured in these muscles was considered as a proxy for ECR and FCR reflex activity. Muscle tone in the arm was categorized by: hypo-, normo- and hypertone. The clinical assessment were usually performed on the same day. In the event that same day assessment was not possible, the results from the closest neurological exam was then chosen.

2.4 Signal preprocessing

Recorded wrist torque, EMG and angle measurements were stored at a sample frequency of 2048Hz. The recorded EMG signal were bandpass filtered between 20Hz and 450Hz (3^{rd} order Butterworth). The filtered EMG was rectified and normalized to the EMG recordings during maximum voluntary contraction (MVC). EMG of the FCR and ECR were combined resulting in one EMG signal. EMG is combined in one signal to obtain a linear relation between EMG and wrist angle. Then, the recorded and processed signals were resampled at 128Hz to reduce computational load. The first 3s and the last 2s from all the measured signals were removed to reduce the influence of transient effects caused by the start or end of the perturbations sequence[19].

2.5 The experiment

A protocol designed by Mugge et al.[19] was adapted and expanded with additional tasks. EMG was normalized to allow for inter-subject comparison, for this purpose the EMG at rest and during MVC were used. First the EMG activity of the arm at rest was measured. After the baseline measurement we recorded the MVC of the FCR and ECR with a handheld dynamometer (MicroFET, Hoggan Scientific, United States, Utah, Salt Lake City). The MVC was recorded 3 times in both directions yielding 6 measurements in total, each lasting 6 seconds. After the initial MVC measurements, 3 main tasks were performed. During these tasks continuous torque perturbations were applied to the participants right wrist. These tasks were:

1. Relax task (RT) , minimize muscle activity to ensure passive behavior .
2. Force task (FT), maintain a bias force by complying with the perturbations.
3. Position task (PT), maintain position by resisting the perturbations.

Force tasks were performed with a bias level of 5% and 10% of the obtained MVC applied to the handle. At the start of each task the task was explained in depth and practiced prior to recording. The recorded measurements started when the performance of the participant was deemed adequate and when the deviation of the wrist angle was between 1.0° from the reference position. Each task was recorded 3 times for averaging purposes, thus yielding 12 trials in total per subject. After the 3 recorded measurements the next task was explained and practiced. The tasks were performed in the following order: RT, $FT_{5\%}$, $FT_{10\%}$, PT.

2.6 Perturbation signal

The perturbation signal used was a so called multisine signal. A multisine consists of a sum of sine functions. The perturbation signal was designed in the frequency domain according to the reduced power method[20]. Briefly, the signal contained a rectangular spectrum with dominant power from 0.1Hz to 0.7Hz and signal was supplemented with reduced power from 0.7Hz to 40Hz. Power was applied to two adjacent frequency points to enable frequency averaging. Inverse Fourier transformation yielded unpredictable time signals with a duration of 37s. This method allows for more robust estimation of high frequency dynamics and corresponding parameter estimation, while still evoking behavior adapted to low frequent perturbations[20]. The amplitude of the dominant power signals was scaled to obtain a standard deviation of the wrist angle of approximately 1.0°, to avoid non-linear behavior. The reduced power frequencies were left unaltered to ensure a good signal–to-noise ratio (SNR).

2.7 Non-parametric analysis

Differences between perturbation and response, obtained from the closed-loop SI approach, were estimated with frequency response functions (FRF)[6,9-12,23]. A FRF expresses the difference between input and output in terms of the amplitude (gain) and the delay (phase)[24]. Two different FRFs were estimated from the measured signals. The first FRF describes the joint admittance, the compliance of the limb to disturbances. A decrease of the joint admittance indicates an increase in the force required to displace the limb. The second FRF describes the reflexive impedance, the muscle activity in response to limb displacement. The resulting FRF were estimated as follows[6]:

$$\hat{H}_{T\theta}(f) = \frac{\hat{S}_{d\theta}(f)}{\hat{S}_{dT}(f)} \quad (1)$$

$$\hat{H}_{\theta a}(f) = \frac{\hat{S}_{da}(f)}{\hat{S}_{d\theta}(f)} \quad (2)$$

Where $\hat{H}_{T\theta}(f)$ denotes the estimated joint admittance and $\hat{H}_{\theta a}(f)$ the estimated reflexive impedance. The FRFs are calculated from the cross-spectral density that are denoted by $\hat{S}_{d\theta}(f)$, $\hat{S}_{dT}(f)$ and $\hat{S}_{da}(f)$, with *d*, *θ*, *T* and *a* denoting the perturbation, wrist angle, wrist torque and the combined EMG from the flexor and extensor. The frequency vector is denoted by *f* and contains all the frequencies where the perturbation signal contained power.

The non-parametric procedure assumes no predefined model structure, except for linearity[25]. Coherence was determined as a measure of linearity and noise. The coherence for the admittance and the reflexive impedance are given by the following equations[6]:

$$\hat{\gamma}_{d\theta}{}^2(f) = \frac{|\hat{S}_{d\theta}(f)|^2}{|\hat{S}_{dd}(f)^2\hat{S}_{\theta\theta}(f)^2|} \quad (3)$$

$$\hat{\gamma}_{da}{}^2(f) = \frac{|\hat{S}_{da}(f)|^2}{|\hat{S}_{dd}(f)^2\hat{S}_{aa}(f)^2|} \quad (4)$$

Where $\hat{S}_{dd}(f)$, $\hat{S}_{aa}(f)$ and $\hat{S}_{\theta\theta}(f)$ are the auto-spectral densities of the perturbation signal, measured EMG and the wrist angle θ. Coherence ranges from 0 to 1, with 1 indicating a perfect linear system with no noise present.

2.8 Parametric analysis.

To obtain physiological relevant parameters a NMM was fitted to the data. The NMM implemented was described by Schouten et al[11]. The output of the model is determined by 13 parameters, of which 8 are condition dependent and 5 are condition independent. The parameters and their boundaries are given in table 1. The condition independent parameters include inertia (I), time delay for the GTO and MS (T_{ms}, T_{gto}), bandwidth of the activation dynamics (f_a) and relative damping of the activation dynamics (β_a). The 8 condition dependent parameters capture the properties of the intrinsic and reflexive pathways and the contact dynamics. Intrinsic muscle stiffness k and the muscle viscosity b are related to intrinsic muscle contraction. The contribution of the proprioceptive reflexes was expressed by 3 parameters in the NMM: response of muscle spindles and Golgi tendon organs to muscle stretch (II afferent), stretch rate (Ia afferent) and muscle force (Ib afferent). Effect of the contact between handle and hand was captured by an additional viscoelastic component and was expressed by the stiffness (k_c) the viscosity (b_c). The final condition independent parameter was the tendon stiffness (k_{tend}). The parameters were estimated simultaneously for each individual participant, resulting in a total of 37 parameters per participant. Estimation of the parameters was done by minimizing an error function. This is described in detail in appendix A.

Table 1 The parameters derived during the parameter estimation. The initial value for the parameters and their upper and lower boundaries are given.

Parameters	Initial value	Lower boundary	Upper boundary
Wrist inertia, I (kgm^2)	0.005	0.001	0.01
Muscle spindle time delay, T_{ms} (ms)	0.04	0.02	0.06
Golgi tendon organ time delay, T_{gto} (ms)	0.03	0.02	0.06
Eigen-frequency activation dynamics, f_a (Hz)	3	2	10
Relative damping activation dynamics, β_a (-)	0.75	0.5	2
Contact dynamics viscosity, b_c (Nms/rad)	2	0.01	5
Contact dynamics stiffness, k_a (Nm/rad)	10	1	100
Tendon stiffness, k_{tend} (Nm/rad)	100	50	1000
Muscle viscosity, b (Nms/rad)	0.06	0.0001	2
Muscle stiffness, k (Nm/rad)	4	1	30
Muscle stretch velocity feedback gain (Ia afferent), K_v (Nms/rad)	0.1	-5	5
Muscle stretch length feedback gain (II afferent), K_p (Nm/rad)	1	-10	10
Golgi tendon organ force feedback gain (Ib afferent), K_f (-)	0	-2	2

2.9 Internal and external validation

Internal validation was performed by examining the sensitivity of the parameters on the fitting error. High sensitivity indicates that a small change of the parameter leads to a large change on the fitting error. Sensitivity was expressed by the standard error of the mean (SEM), a low SEM indicates a high sensitivity. High sensitivity indicates that a parameters has an observable contribution in the system's response and is estimated with certain accuracy. External validation of the model was based on variance accounted for (VAF). A VAF of 100% indicates that the behavior is completely described by the model:

$$VAF = \left(1 - \frac{\sum(X_{meas}(t) - X_{model}(t))^2}{\sum X_{meas}(t)^2}\right) \cdot 100\% \qquad (7)$$

Where $X_{meas}(t)$ is the measured wrist torque or angle, $X_{model}(t)$ is the torque or angle estimated by the model. Resulting in VAF_θ (wrist angle) and VAF_T (wrist torque).

2.10 Statistical analysis

Normal distributed variables were described as mean (SD), whereas median [IQR] was used for non-normal distributed variables. Normal distributed variables included: the neuromechanical parameters, age of the subjects and the MVC of the subjects. Non-normal distributed variables included: ALSFRS-R score ,FMF scores and VAF values. Normality was tested with Shapiro-Wilk test. Differences in clinical characteristics and neuromechanical parameters were assessed with Wilcoxon rank-sum test, Student's t-test and Chi-Square test for non-normal distributed, normal distributed and categorical data, respectively. A separate measure, termed low frequency admittance (LFA), was devised to compare FRFs of patients directly, rather than through model parameters. LFA was calculated by averaging the admittance in the 0.1-0.7 Hz bandwidth, as the perturbation signal had dominant power there. Association between LFA and strength was assessed using Spearman rank correlation. Furthermore, the medians of the LFA were compared between tasks with Wilcoxon rank-sum test. Neuromechanical parameters are compared between patients and controls. For all statistical tests $p<0.05$ was deemed significant. All statistical analyses were performed in R. MATLAB was used for signal processing, parameters estimation and validation of the model.

3 Results

3.1 Participants

Characteristics of the study population are presented in Table 2. Participant populations were matched by gender with controls being 11 years younger on average. Recorded MVC was lower in ALS patients than in controls. 11/15 (73%) of the patients had elevated or pathologic reflex activity in the right arm. 13/15 (87%) of the patient group had normal muscle tone in the right arm. MRC scores of the FCR in all patients was 5 out of 5. 3/15 (20%) had a MRC score of 4 in the ECR, the rest of the patients had a MRC of 5 in the ECR. 13/15 (87%) of the patients received Riluzole (50mg, 2 per day) at the time of participation. Riluzole is a neuroprotective drug which inhibits glutamate release in the CNS[26], it is commonly prescribed for ALS patients. All participants were able to perform the different tasks. The RT and PT were generally well performed, with only 1 training trial required. However, during RT participants with low MVC had large deviations of the wrist angle. To correct for these deviations, we notably decreased the dominant power of the perturbation signal until the standard deviation of the wrist angle was around 1°. One participant requested more rest between the different measurements during the PT. The FTs were the most difficult tasks and generally required 2-3 training trials before the participants were able to comply with the perturbations. Additionally, one patient exhibited fasciculations (spontaneous muscle twitches) over the upper arm (triceps) during all the tasks. Figure 2 depicts a representative measurement, i.e. the recorded angle of- and torque on-the wristalyzer handle, of a control and a patient with MRC 5 on the FCR and ECR.

Table 2 Characteristics of the study population.

Clinical measures	ALS (n=15)	Controls (n=15)	P
Gender- Male	8	8	
Age years (mean, SD)	63.8 (5.3)	52.1 (12.2)	0.001
Summed MVC (mean, SD)	15.0 (3.9)	18.8 (4.6)	0.003
Reflex scores (normal/ elevated/pathological)	4/8/3[a]	-	
Muscle tone scores (hypo-/ normo-/ hypertone)	1/13/1[a]	-	
ALSFRS-R (median, IQR)	41 [38-42]	-	
FMF (median,IQR)	7 [7-8]	-	

a. The numbers represent the amount of patients that were diagnosed with the respective clinical scores for reflexes and muscle tone.

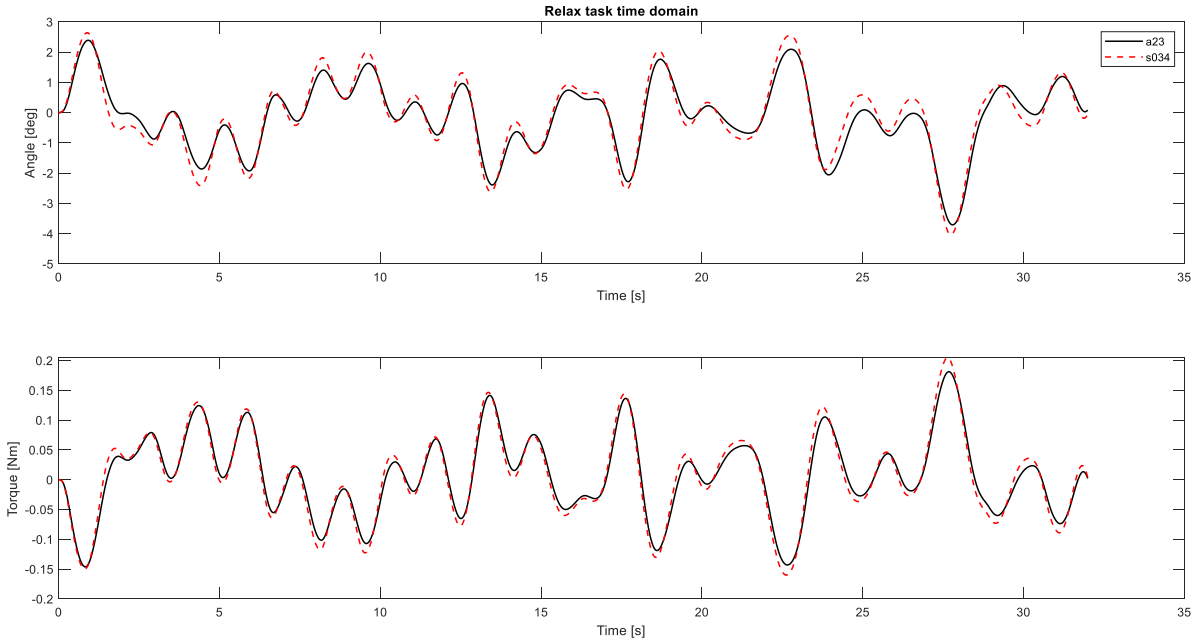

Figure 2: Time domain signal of the handle position and the torque on the handle between a patient (a23) and a control (s034) of comparable strength. The top graph show the deviation of the angle from the starting point. And the bottom graph show the torque exerted on the handle. The signals were filtered with a 3rd order Butterworth filter at 3 Hz.

3.2 Analyses of the joint admittance

From the measurements the FRFs for the joint admittance and reflexive impedance were estimated. Perturbation levels were altered for each task. In the FTs the participants were subjected to lower perturbations levels, where the dominant power signal was initially set so that the reduced power was 20% of the dominant power signal. In the RT and the PT the reduced power was 2% of the dominant power. The perturbation level could be altered to ensure linear behavior. Figure 3 displays the admittances of the patients compared with the averaged admittance of the controls. The highest average LFA was observed during the RT ($\hat{H}_{T\theta}$ = 0.63). LFA in the FTs was lower ($\hat{H}_{T\theta}$ = 0.22 and $\hat{H}_{T\theta}$ = 0.16) for the $FT_{5\%}$ and the $FT_{10\%}$ respectively. LFA was lowest during PT ($\hat{H}_{T\theta}$ = 0.09). Please note that LFA, and admittance in general, is provided on a log-10 scale by convention.

3.2.1 Relax task

Figure 3A depicts the admittance of the RT. The patient group had large variance in the admittance (σ^2=0.6) compared to controls (σ^2=0.27). LFA of the patients was higher compared to controls ($p<0.05$). Gender had a large influence on the LFA, in the control group women had higher admittance compared to men ($p<0.05$). Muscle strength, indicated by MVC, was negatively associated with admittance in the LFA in the group of ALS patients (ρ = -0.71, $p< 0.01$), yet no such association was found in controls.

3.2.2 Force tasks

Admittance during the FTs is presented in figures 3B-C. The LFA during both FTs were significantly lower than in RT ($p<0.01$). Notably, no difference was observed in the LFA of patients and controls. In $FT_{5\%}$ patients had more variability in their admittance at the lowest frequency than in $FT_{10\%}$ (σ^2 = 0.06, σ^2 = 0.01). In $FT_{10\%}$ MVC was negatively associated with admittance (ρ =-0.64, $p<0.05$) in the control group, in the ALS patients no such association was found.

3.2.3 Position task

Admittance during the PT is depicted in figure 3D. Notably the controls were able lower their admittance compared to patients in the LFA, a significant difference was found ($p<0.05$). A correlation between MVC and admittance was found in controls (ρ =-0.68,$p<0.001$), yet no such correlation was found in patients (ρ=0.11,p=0.7).

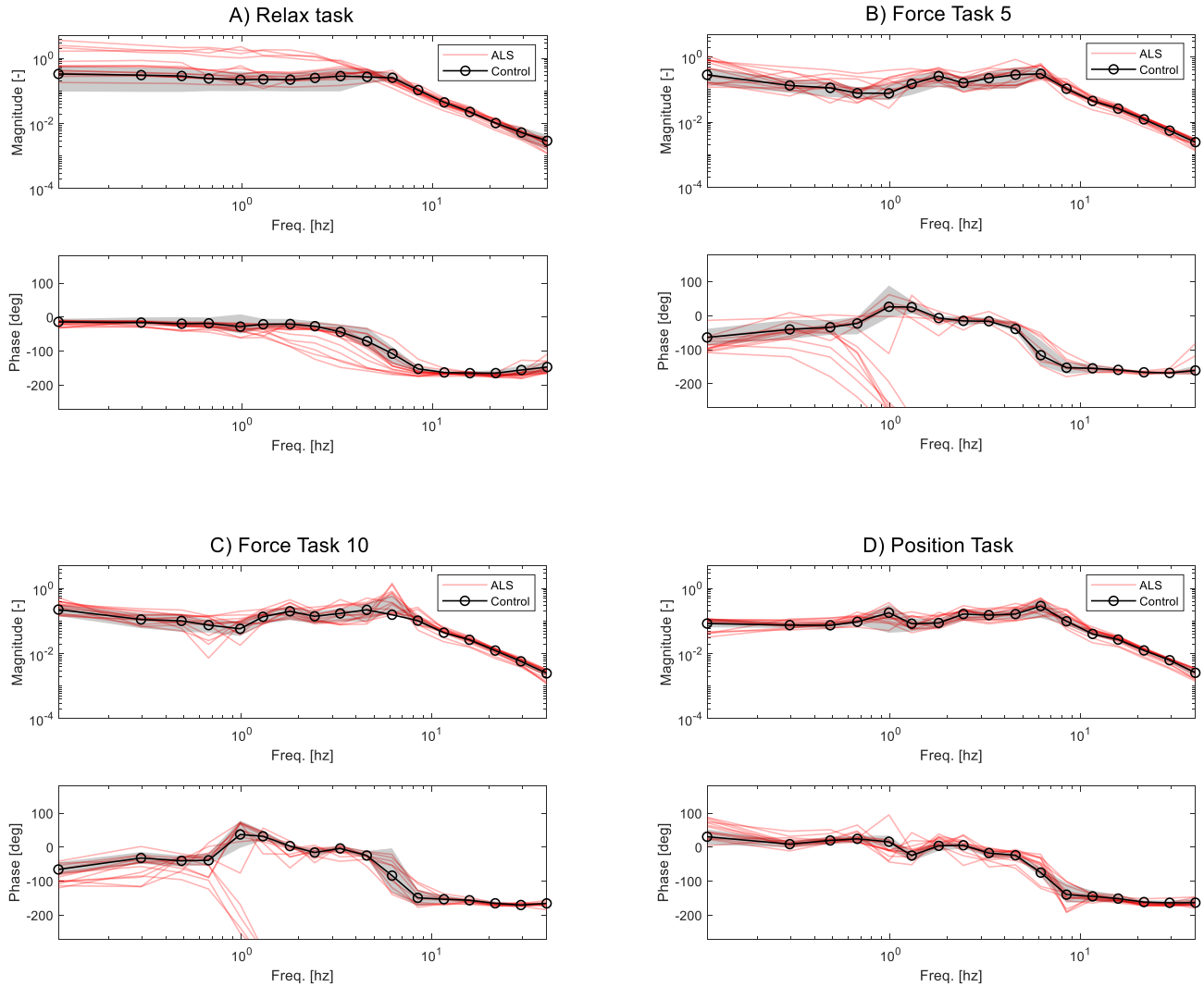

Figure 3: FRFs of individual patients (red lines) and averaged FRFs of controls (black line, shaded area depicts SD). Admittance and phase during A) the relax task, B) the force task with a 5% bias force. C) the force task with a 10% bias force and D) the position task. Of note, the phase of some patients during the FTs a sharp drop can be observed. This is caused by the unwrap function in MATLAB.

3.3 Quality of the FRFs

Generally, the measurements were linear and the SNR was high, as indicated by the coherence (γ^2) in each individual. Averaged over all frequencies, coherence for the patient group was: RT (γ^2= 0.96 (0.09)), $FT_{5\%}$ (γ^2= 0.95 (0.10)), $FT_{10\%}$ (γ^2= 0.96 (0.09)) and PT (γ^2= 0.95 (0.10)). In the control group the averaged coherence were : RT (γ^2= 0.98 (0.04)), $FT_{5\%}$ (γ^2= 0.94 (0.13)), $FT_{10\%}$ (γ^2= 0.95 (0.12)) and PT (γ^2= 0.96 (0.07)). RT had the highest average coherence and in all participants the coherence was $\gamma^2 > 0.7$ for all frequencies. In the FTs and PT a dip in coherence was observed between 0.5-1.5Hz. This is likely caused by the attempt to correct for higher frequency disturbances. In $Ft_{5\%}$ this dip was below $\gamma^2 = 0.7$ in 5/15 (33%) patients and 5/15 (33%) controls, in $FT_{10\%}$ 4/15 (27%) patients and 4/15 (27%) controls and 4/15 (27%) patients and 2/15 (13%) controls in the PT.

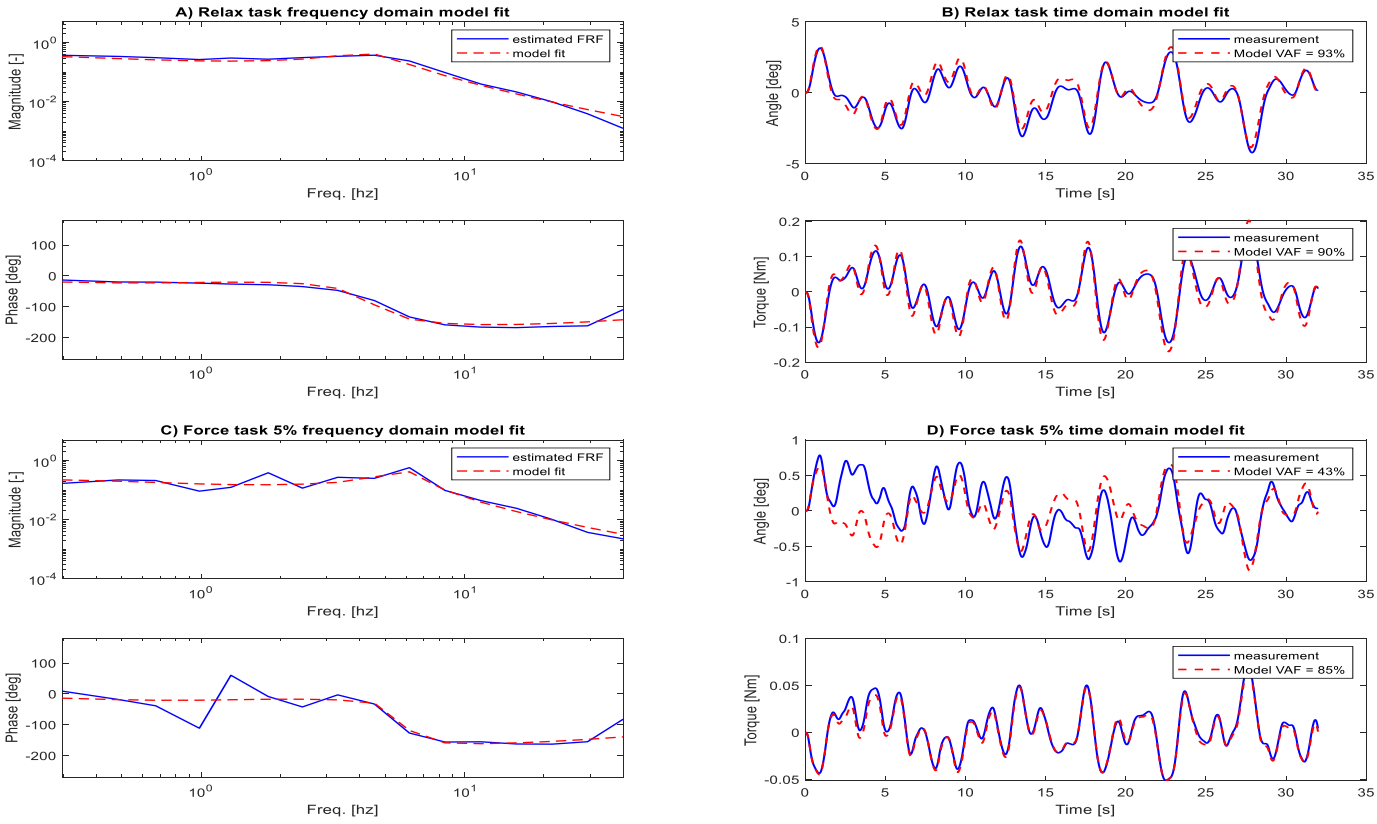

Figure 4: The validity of the model in both frequency and time domain. And the box plot of the intrinsic and reflexive parameters. A) The model fit on the estimated admittance (top panel) and the phase (bottom panel) of a single subject during the relax task. B) Model fit in the time domain with the angle of the handle (top panel) and the torque on the handle (bottom panel) during the relax task. C) Model fit on the estimated admittance (top panel) and the phase bottom panel for the $ft_{5\%}$. D) The model fit in the time domain during the $FT_{5\%}$. The VAF values are high meaning the model has a good external validity.

3.4 Goodness of the fit

The SEM values of the parameters were calculated from the covariance matrix. Most SEM values of both controls and ALS were below 10%, indicating that the parameters had high sensitivity. The SEM value of the velocity feedback gain (k_v) of all tasks was higher than 10%. External validation was performed using VAF as measure. The VAF of the torque was highest in the PT and lowest in the two FTs. Median VAF_T for all individuals were: RT=99% [92-100%], $FT_{5\%}$=94% [89-98%], $FT_{10\%}$=98% [93-99%] and PT=99% [99-100%]. Median VAF_θ of all individuals were: RT=95% [86-99%], $FT_{5\%}$= 85% [65-96%], $FT_{10\%}$= 94% [58-99%] and PT= 95% [88-98%]. The median VAFs were high during all tasks however in the FTs the VAF_θ had larger variance than in RT and PT. VAF_T was high during all tasks. In two controls unreasonable values of VAF_θ were found during the FTs, one in $FT_{5\%}$ and one in $FT_{10\%}$. Two ALS patients had unreasonable VAF_θ values during $FT_{10\%}$. These values were excluded. The VAF values of the patient and ALS groups are represented in table 3. Figure 4 shows the model fit of one patient for the RT and $FT_{5\%}$ in both time and frequency domain.

Table 3 VAF values for the control and ALS group.

Task	Wrist torque VAF_T, median [Q1-Q3]				Wrist angle VAF_θ, median [Q1-Q3]			
	RT	$FT_{5\%}$	$FT_{10\%}$	PT	RT	$FT_{5\%}$	$FT_{10\%}$	PT
ALS	98% [91-99%]	95% [89-98%]	96% [94-99%]	99% [99-100%]	92% [80-97]	83% [75-96%]	92% [61-98%]	97% [89-99%]
Control	99% [98-100%]	94% [81-98%]	98% [90-99%]	99% [99-100%]	97% [86-99%]	85% [48-99%]	92% [46-99%]	94% [88-98%]

3.5 Comparison in intrinsic and reflexive parameters between patients and controls

Figure 5 compares the neuromechanical parameters for the control and the patient groups for each task. The viscosity and stiffness of the muscles for controls and patients are shown in figure 5A-B. Surprisingly the stiffness and viscosity in the patient group were not significantly different from the control group. The reflexive parameters, type Ia, II afferents from the MS and type Ib afferent from the GTO, are shown in figure 5C-E. During the RT the reflexive parameters were located around zero. In the active tasks, the reflexive feedback is increased as can be seen in figure 4C-E. Surprisingly the patients have similar reflexive feedback compared to controls in most tasks, except for the FTS. Patients had more inhibitory position feedback in (k_p = -1.5 Nm/rad, $p < 0.05$) in $FT_{5\%}$, more inhibitory velocity feedback (k_v = -0.2 Nms/rad, $p < 0.001$) and more excitatory force feedback (k_f = -0.7, $p < 0.001$) compared with controls. Table 2 shows the values of the 5 condition dependent parameters for each task.

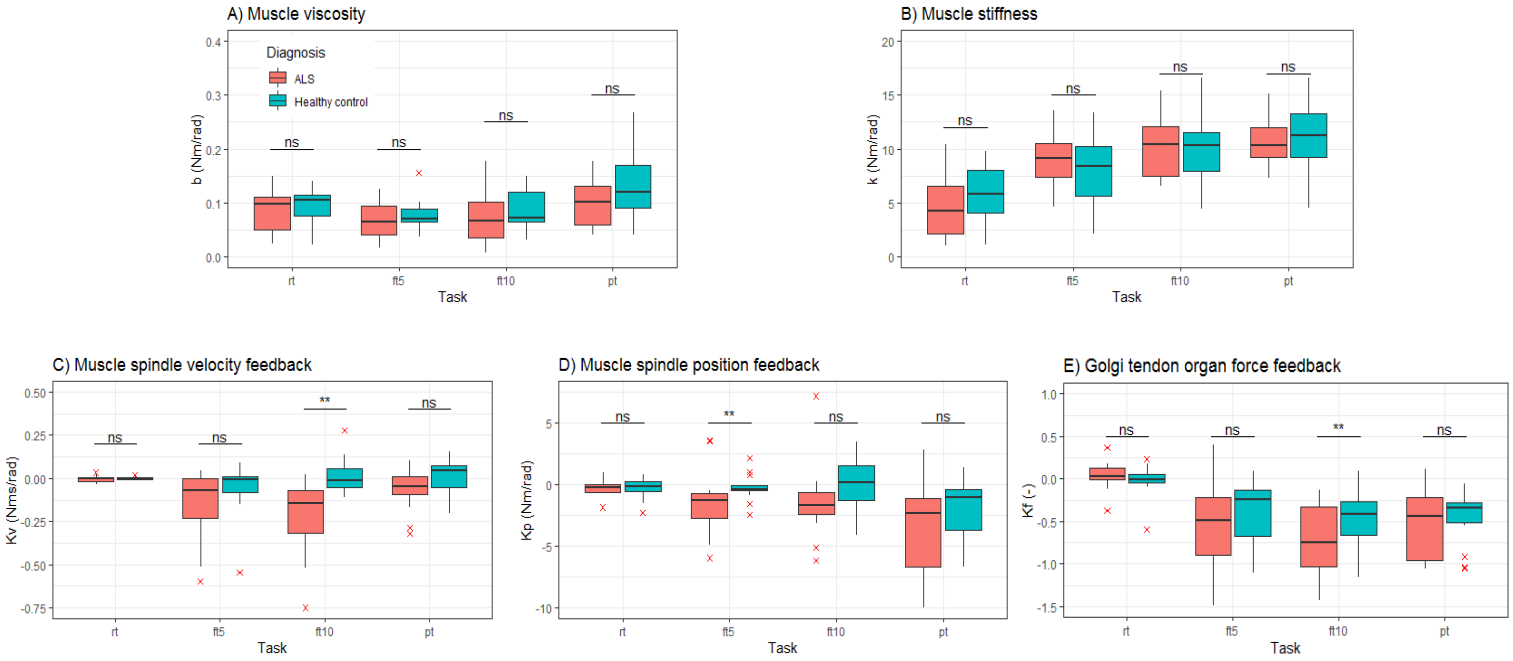

Figure 5: The neuromechanical parameters depicted in box plots with the patients in red and the controls in blue. With A and B depicting the intrinsic parameters and C-E the reflexive parameters. A) The boxplots of the muscle viscosity (b) for all 4 tasks. B) The muscle stiffness (k). C) the muscle spindle velocity feedback gain (k_v). D) muscle spindle position feedback gain (k_p). E) Golgi tendon organ force feedback (k_f).

3.6 Comparison with clinical measures.

No relationship was found between the ALSFRS-R scores and the FMF score with respect to the neuromechical parameters. Because the muscle tone groups were too small no relationship could be determined. However, a relationship was found in the different scores of reflex activity. Our hypothesize were a relation between the reflexive parameters and reflex scores during the RT was not found. But in the active tasks clear differences were observed in patients with increased reflex activity. The neuromechanical parameters grouped by clinical score for reflex activity in the active tasks (FTs, PT) are shown in figure 6. In figure 6 differences can be observed between different levels of reflex activity. This is most notable in the group with pathologically increased reflexes. Due to the correlation between the FRFs and gender and MVC we corrected for these covariates. Linear regression was used for each of the neuromechanical parameters from the data of the healthy controls with MVC and gender as covariates. The linear model was then used to predict the value of the parameter for all participants. These values were subtracted from the measured values and divided by the residuals from the linear model of the healthy controls. Resulting in standardized values where the mean of the controls is 0 and the values of the patients indicate the deviation from the mean, the z-scores. However, the relation between the parameters and the reflex groups remained similar. Indicating that the obtained results are reliable even in weaker patients.

3.6.1 Neuromechanical parameters in patients with pathologically increased reflexes.

Patients with pathologically increased reflexes had increased inhibitory MS feedback (k_v and k_p) and increased excitatory GTO feedback (k_f) in the FTs, stiffness (k) was increased in all active tasks. Patients with pathologically increased reflexes had significantly more inhibitory velocity and position feedback (k_v =-0.27, k_p =-4.6) compared to controls (k_v =-0.0008, k_p =-0.3) in $FT_{10\%}$ ($p < 0.05$). Force feedback was significantly more excitatory in patients with pathologically increased reflexes (kf = -1.1) compared to controls (kf = -0.47,$p<0.05$). In $FT_{5\%}$ position dependent feedback was was significantly more inhibitory (k_p = -4.9 Nm/rad) compared to controls (k_p = -0.22 Nm/rad,$p < 0.05$). Notably, stiffness was significantly increased during all the active tasks compared to controls ($p<0.05$). These findings indicate that the neuromechanical parameters are sensitive to clinical measures of UMN degeneration, for which increased reflexes is a classical sign.

3.6.2Neuromechanical parameters in patients with elevated reflexes

Patients with elevated reflexes had increased inhibitory position feedback (k_p=-1.6 Nm/rad) in the $FT_{5\%}$ compared to controls (k_p=-0.22 Nm/rad, $p<0.05$) and in the $FT_{10\%}$ velocity feedback (k_v = -0.11) was significantly more inhibitory than in controls (k_v =-0.0008, $p<0.05$).

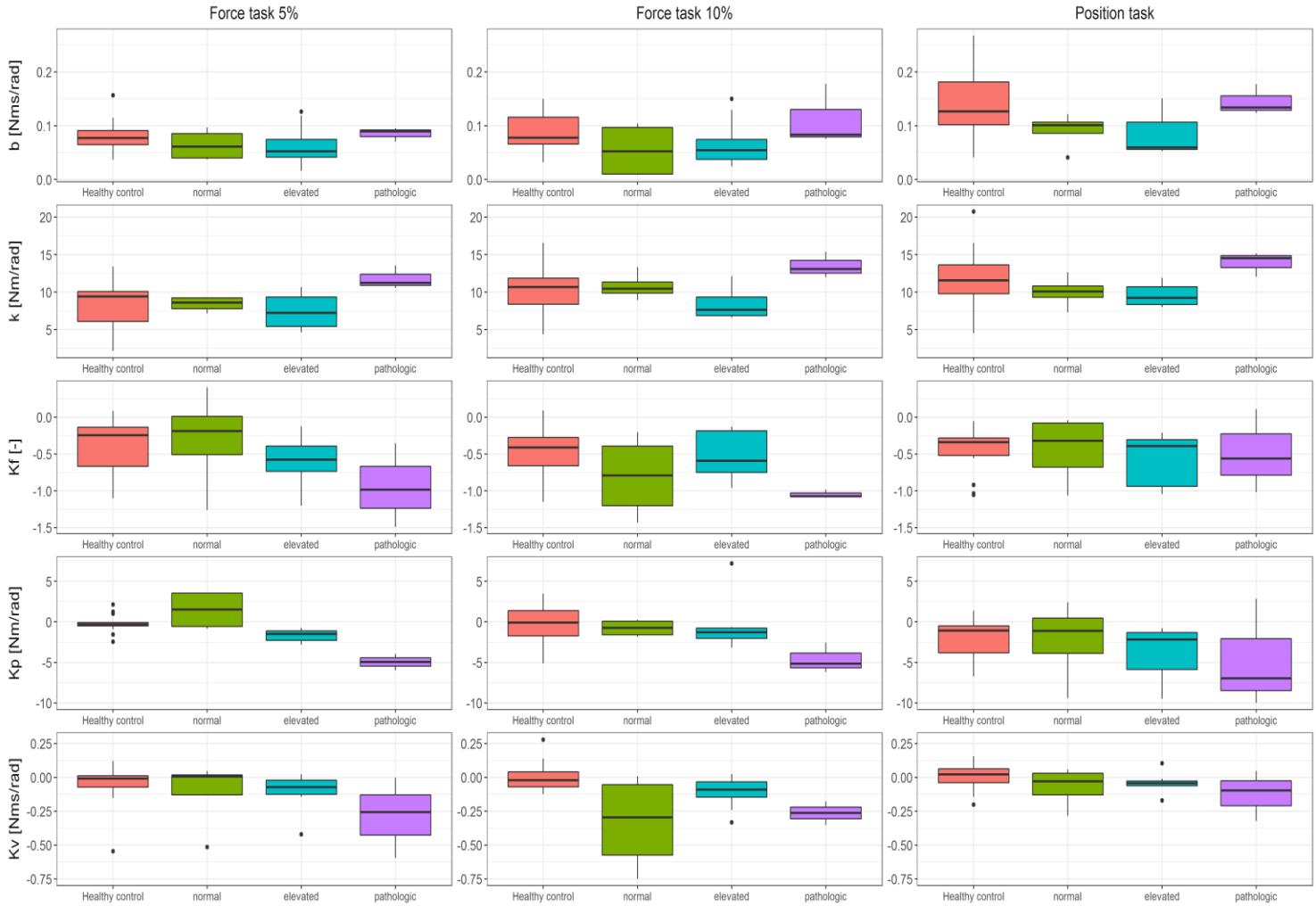

Figure 6: Box plots of neuromechanical parameters for the active tasks. The panels present the $FT_{5\%}$, $FT_{10\%}$ and PT from left to right. Inside the panels on the x-axis the 4 levels of reflex activity are shown. The different scores for reflex activity are: red for healthy controls, green for normal reflexes, blue for elevated reflexes and purple for pathologic reflexes.

4 Discussion

We used closed-loop system identification techniques and parameter estimation to explore if UMN degeneration is detectable in the neuromechanical parameters of ALS patients. The method makes use of a robot to apply continuous force perturbations to the wrist. System identification and a neuromuscular model are used to express the estimated joint dynamics in physiologically relevant neuromechanical parameters. Joint dynamics of the right wrist were estimated in both a relaxed state and in active states. Intrinsic and reflexive parameters were compared between patients and controls and compared with clinical measures. We hypothesized that the reflexive parameters, pertaining to the feedback of the type Ia and II of the MS and type Ib of the GTO, were closely related to the neurological examination in the RT. No correlation was found in the RT but during FTs the parameters were responsive to clinical scores of reflex activity, which is an indication of UMN degeneration.

4.1 Validity

High average coherence in the participants indicate that the behavior had a high SNR and that behavior can be considered linear. Therefore, the use of a linear model was justified. The VAF values indicate how good the model describes the measurements. Both the wrist angle and the wrist torque were well described by the model in the RT and PT, indicated by the high VAF values. Wrist torque was well described in the FTs. Wrist angle however had lower VAF values in the FTs and large variance. During FT the objective is to maintain a force and give way to force perturbations allowing variations in the angle of the handle.

4.2 Measurements

Different tasks required the participants to elicit different control strategies in order to comply with the task. All participants were able to perform the protocol, during the experiment only 1 patient requested some more time during the position tasks indicating that the protocol was not too demanding for most patients. The RT and PT were well-performed requiring minimal training. FTs were less intuitive and required more training. Adapting the power of the perturbation signal allowed the protocol to be used in a group with large strength differences. Patients and controls could only be differentiated in the FRFs during the RT, where the average admittance of the ALS patients was visibly higher compared to the controls. However during the different tasks both patients and controls were able to alter their admittance to comply with the task instruction.

4.2.1 Relation between admittance and MVC

Admittance of patients in the RT was negatively associated with MVC, in the PT however no such association was found. The control group had the opposite no association in the RT between admittance and MVC and in PT there was a negative association. During the position tasks participants are instructed to resist all perturbations. The best approach for this is to use co-contraction thereby increasing the intrinsic stiffness. Stronger participants would be able to better resist the perturbations thereby decreasing their admittance the most, as was observed in the healthy controls. A possible explanation is that ALS patients fatigue faster than controls. Large motor neuron death in ALS leads to reinnervation of fast type muscle fibers by smaller motor neurons, these fatigue faster. Although the muscle fiber are changed to slow-type fibers the change is often incomplete[37], causing patients to fatigue faster. Fatigue in ALS might be caused by dysfunction of corticospinal motor neurons (UMN) that leads to reduced voluntary muscle activation or degeneration of the LMNs leads to an inability of the motor units to sustain muscle activity. It remains unclear whether fatigue in ALS is caused by UMN or LMN degeneration, with studies finding evidence for both[38-40]. Weakness was not related to fatigue in ALS[40]. Therefore, it is possible that due to fatigue some patients were not able to use all their strength during the task to lower their admittance.

4.3 Reflexive parameters

The reflexive parameters found in this study are in accordance with previous studies. The reflexive parameters in the RT are around zero. In the PT MS velocity feedback k_v and position feedback k_p were found to be inhibitory, where the force feedback from the GTO k_f was found to be excitatory[6,10,20]. The force dependent feedback of the GTO k_f in the FTs was found to be excitatory, where a previous study found the k_f inhibitory during the FT[20]. However in this study the FTs were implemented with a bias force, whereas the previous study had no bias force during the FT.

4.4 Relation of neuromechanical parameters to clinical scores of reflex activity.

4.4.1 Hyperreflexia

The patients with pathologically increased reflexes showed increased inhibitory velocity and position feedback (k_v, k_p) and increased excitatory force feedback (k_f) compared to controls. The increase in reflexive feedback drives the system to instability, to counteract this the patients increase their stiffness. Hyperreflexia is associated with the decrease of supraspinal control to the spinal reflexes. This loss of supraspinal control leads to less modulation of the afferent feedback. Thereby increasing the feedback gain which increases the excitability of spinal reflexes[42]. UMN dysfunction in ALS is associated with reduced corticospinal inhibition[43]. This can be seen in the patients with pathologically increased reflexes during the FTs.

4.4.2 Normal reflexes

In the patients with normal reflex activity the difference with the control group were small and no significant difference was found. Apparently these patients are able to perform the tasks comparably to a healthy control. An explanation for this is the heterogeneous nature of ALS. In these patients the arm might not yet be affected or is only minimally affected. This was further supported by the fact that these patients had normal muscle tone and high MRC scores for the FCR and ECR. Interestingly during the FTs there was one outlier, this patient had a neurological exam on the day of the experiment were the reflexes in biceps and triceps were marked as normal. However, during a neurological examination on a later date the reflexes in this patient were marked as pathological increased reflexes. The results show that this patient had the same behavior as patients with pathologic increased reflexes. Apparently the reflexive parameters were able to correctly identify this patient, or are more sensitive and therefore able to predict the reflexive score more accurately. Testing of the reflexes is shown to have high variance between observers[41]. Therefore, it is more likely this patient was scored incorrectly.

4.5 Clinical implication

The results of the present study indicate that increased reflex activity can be measured during active tasks. Currently in ALS hyperreflexia is measured by eliciting the monosynaptic reflex (Ia afferent), the method used in this study provides a measure for assessing the polysynaptic reflex (Ib-II afferent) as well as the monosynaptic reflex. Reduced recurrent inhibition is observed in ALS which leads to increased excitability of the Ia afferent[45]. In a recent study in mice it was shown that ALS affects the type Ia and type II afferents[44]. Furthermore, it is proposed that an imbalance between α- motor neurons and γ-motor neurons in ALS which would lead to increased MS afferent activity[46]. However, no evidence was found that the Ib afferents are affected by ALS. In this study patients with pathologic increased reflexes had overexcited type Ib and type II afferents during the FT. These findings suggest that hyperreflexia in ALS is associated with increased feedback from the GTO as well as increased feedback from the MS. The method proposed in this study can be a useful tool to better monitor the mechanisms of hyperreflexia in ALS.

4.6 Limitations

4.6.1 Linearity

The assumption of linearity is a limitation. In order to achieve linearity the movements are kept small. The type II or type Ib (k_f, k_p) afferents are more sensitive to a larger range of motion than the type Ia afferents (k_v)[29]. Meaning that hyperreflexia would only be revealed during significant length changes. Due to the small movements in order to achieve a linear response this might explain why there is no differentiation between patients with increased reflexes during the RT. However in the active tasks the type Ib and type II afferents show increased excitability. Active tasks requires the participant to mainly rely on their reflexes for the FTs and during PT to rely on co-contraction. As previous studies show the different control strategies during active tasks lead to increased feedback gain from the proprioceptors[20]. It remains difficult to interpret the results from the active tasks since there are no comparable metrics, because most examinations are done with the limb at rest.

4.6.2 Small study group

Another limitation was the small study group. The group of patients that participated in this study was small and possibly did not cover the entire clinical spectrum. For instance only 2 patients had altered muscle tone in their arm. One patient where the muscle tone was increased (hypertone) and one with reduced muscle tone (hypotone). Therefore, no relation was observed between muscle tone and neuromechanical parameters.

5 Conclusion

The current study explored the application of closed-loop system identification and parameter estimation in ALS. The goal was to relate clinical examinations of UMN degeneration with physiologically relevant neuromechanical parameters.

Patients were able to alter their joint dynamics to comply with the task. We found that during the relax task patients had visibly higher admittance than controls. In the active tasks the force tasks and position tasks patients were able to lower their admittance comparable with controls. However, patients were not able to use all their strength to resist the perturbations during the position task, possibly because of fatigue.

Neuromechanical parameters were not able to indicate a difference between patients and controls. However, reflexive parameters in the force tasks were significantly increased in patients scored with pathologic reflexes, which is an indication of hyperreflexia. Position feedback of the muscle spindles and force feedback of the Golgi tendon organ were increased in patients with hyperreflexia. Indicating that hyperreflexia in ALS also affects the type II and Ib afferent.

To conclude the proposed method is able to identify patients with hyperreflexia, a sign of UMN dysfunction, in the reflexive parameters during active tasks. Therefore, it could be an useful tool to monitor disease progression of ALS and potentially be used to observe the effect of medication on hyperreflexia in ALS. In this study the right wrist was used but the proposed method can be used on different limbs, such as the ankle.

Bibliography

1) van Es MA, Hardiman O, Chio A, Al-Chalabi A, Pasterkamp RJ, Veldink JH, van den Berg LH. Amyotrophic lateral sclerosis. Lancet. 2017 Nov 4;390(10107):2084-2098. doi: 10.1016/S0140-6736(17)31287-4. Epub 2017 May 25. PMID: 28552366.
2) Traynor BJ, Codd MB, Corr B, Forde C, Frost E, Hardiman OM. Clinical features of amyotrophic lateral sclerosis according to the El Escorial and Airlie House diagnostic criteria: A population-based study. Arch Neurol. 2000 Aug;57(8):1171-6. doi: 10.1001/archneur.57.8.1171. PMID: 10927797.
3) Rowland LP. Diagnosis of amyotrophic lateral sclerosis. J Neurol Sci. 1998 Oct;160 Suppl 1:S6-24. doi: 10.1016/s0022-510x(98)00193-2. PMID: 9851643.
4) Swash M. Hutchison's Clinical Methods. 21st edn. Edinburgh: WB Saunders, 2002:222.
5) Swash M. Why are upper motor neuron signs difficult to elicit in amyotrophic lateral sclerosis? J Neurol Neurosurg Psychiatry. 2012 Jun;83(6):659-62. doi: 10.1136/jnnp-2012-302315. Epub 2012 Apr 11. PMID: 22496581.
6) van der Helm FC, Schouten AC, de Vlugt E, Brouwn GG. Identification of intrinsic and reflexive components of human arm dynamics during postural control. J Neuroscience Methods. 2002 Sep 15;119(1):1-14. doi: 10.1016/s0165-0270(02)00147-4. PMID:12234629.
7) H. van der Kooij, and F. C. T. van der Helm, "Observations from unperturbed closed loop systems cannot indicate causality," Journal of Physiology-London, vol. 569, no. 2, pp. 705-705, Dec 1, 2005.
8) Schouten AC, de Vlugt E, van der Helm FC, Brouwn GG. Optimal posture control of a musculo-skeletal arm model. Biol Cybern. 2001 Feb;84(2):143-52. doi: 10.1007/s004220000202. PMID: 11205351.
9) Schouten AC, Van de Beek WJ, Van Hilten JJ, Van der Helm FC. Proprioceptive reflexes in patients with reflex sympathetic dystrophy. Exp Brain Res. 2003 Jul;151(1):1-8. doi: 10.1007/s00221-003-1420-x. Epub 2003 May 13. PMID: 12743675.
10) de Vlugt E, Schouten AC, van der Helm FC. Quantification of intrinsic and reflexive properties during multijoint arm posture. J Neurosci Methods. 2006 Sep 15;155(2):328-49. doi: 10.1016/j.jneumeth.2006.01.022. Epub 2006 Feb 28. PMID: 16504304.
11) Schouten AC, Mugge W, van der Helm FC. NMClab, a model to assess the contributions of muscle visco-elasticity and afferent feedback to joint dynamics. J Biomech. 2008;41(8):1659-67. doi: 10.1016/j.jbiomech.2008.03.014. PMID: 18457842.
12) van der Krogt H, Klomp A, de Groot JH, de Vlugt E, van der Helm FC, Meskers CG, Arendzen JH. Comprehensive neuromechanical assessment in stroke patients: reliability and responsiveness of a protocol to measure neural and non-neural wrist properties. J Neuroeng Rehabil. 2015 Mar 13;12:28. doi: 10.1186/s12984-015-0021-9. PMID: 25889671; PMCID: PMC4436851.
13) de Vlugt, E., de Groot, J.H., Schenkeveld, K.E. *et al.* The relation between neuromechanical parameters and Ashworth score in stroke patients. *J NeuroEngineering Rehabil* **7,** 35 (2010). https://doi.org/10.1186/1743-0003-7-35
14) de Gooijer-van de Groep KL, de Vlugt E, de Groot JH, van der Heijden-Maessen HC, Wielheesen DH, van Wijlen-Hempel RM, Arendzen JH, Meskers CG. Differentiation between non-neural and neural contributors to ankle joint stiffness in cerebral palsy. J Neuroeng Rehabil. 2013 Jul 23;10:81. doi: 10.1186/1743-0003-10-81. PMID: 23880287; PMCID: PMC3737029.
15) Zetterberg H, Frykberg GE, Gäverth J, Lindberg PG. Neural and nonneural contributions to wrist rigidity in Parkinson's disease: an explorative study using the NeuroFlexor. Biomed Res Int. 2015;2015:276182. doi: 10.1155/2015/276182. Epub 2015 Jan 22. PMID: 25685778; PMCID: PMC4320927.
16) Xia R, Muthumani A, Mao ZH, Powell DW. Quantification of neural reflex and muscular intrinsic contributions to parkinsonian rigidity. Exp Brain Res. 2016 Dec;234(12):3587-3595. doi: 10.1007/s00221-016-4755-9. Epub 2016 Aug 17. PMID: 27534863.

17) Brooks BR, Miller RG, Swash M, Munsat TL; World Federation of Neurology Research Group on Motor Neuron Diseases. El Escorial revisited: revised criteria for the diagnosis of amyotrophic lateral sclerosis. Amyotroph Lateral Scler Other Motor Neuron Disord. 2000 Dec;1(5):293-9. doi: 10.1080/146608200300079536. PMID: 11464847.
18) Grimaldi G, Lammertse P, Van Den Braber N, Meuleman J, Manto M. A New Myohaptic Device to Assess Wrist Function in the Lab and in the Clinic - The Wristalyzer. In: Ferre M, editor. EuroHaptics. Berlin Heidelberg: Springer-Verlag; 2008. p. 33–44.
19) Pintelon R, Schoukens J. System identification: a frequency domain approach.New York: IEEE Press; 2001.
20) Mugge, W., Abbink, D.A., Schouten, A.C. *et al.* A rigorous model of reflex function indicates that position and force feedback are flexibly tuned to position and force tasks. *Exp Brain Res* **200,** 325–340 (2010). https://doi.org/10.1007/s00221-009-1985-0
21) Mugge W, Abbink DA, Van der Helm FCT (2007) Reduced power method: how to evoke low-bandwidth behavior while estimating the full-bandwidth dynamics. In: Proceedings of the IEEE 10th international conference on rehabilitation robotics, 13–15 June 2007, pp 575–581
22) Schouten AC, de Vlugt E, van Hilten JJ, van der Helm FC. Quantifying proprioceptive reflexes during position control of the human arm. IEEE Trans Biomed Eng. 2008 Jan;55(1):311-21. doi: 10.1109/TBME.2007.899298. PMID: 18232375.
23) Schouten AC, de Vlugt E, van Hilten JJ, van der Helm FC. Design of a torque-controlled manipulator to analyse the admittance of the wrist joint. J Neurosci Methods. 2006 Jun 30;154(1-2):134-41. doi: 10.1016/j.jneumeth.2005.12.001. Epub 2006 Jan 24. PMID: 16434105.
24) Meskers CG, de Groot JH, de Vlugt E, Schouten AC. NeuroControl of movement: system identification approach for clinical benefit. Front Integr Neurosci. 2015 Sep 8;9:48. doi: 10.3389/fnint.2015.00048. PMID: 26441563; PMCID: PMC4561669.
25) D. Westwick and R. Kearney, *Identification of Nonlinear Physiological Systems*. New York: IEEE Press, 2003.
26) Doble A. The pharmacology and mechanism of action of riluzole. Neurology. 1996 Dec;47(6 Suppl 4):S233-41. doi: 10.1212/wnl.47.6_suppl_4.233s. PMID: 8959995.
27) Cedarbaum JM, Stambler N, Malta E, Fuller C, Hilt D, Thurmond B, Nakanishi A. The ALSFRS-R: a revised ALS functional rating scale that incorporates assessments of respiratory function. BDNF ALS Study Group (Phase III). J Neurol Sci. 1999 Oct 31;169(1-2):13-21. doi: 10.1016/s0022-510x(99)00210-5. PMID: 10540002.
28) Emos MC, Agarwal S. Neuroanatomy, Upper Motor Neuron Lesion. [Updated 2021 Aug 26]. In: StatPearls [Internet]. Treasure Island (FL): StatPearls Publishing; 2022 Jan-. Available from: https://www.ncbi.nlm.nih.gov/books/NBK537305/?report=classic
29) Dietz V: Proprioception and locomotor disorders. Nat Neurosci Rev 2002, 3:781-790.
30) de Carvalho M. Testing upper motor neuron function in amyotrophic lateral sclerosis: the most difficult task of neurophysiology. Brain. 2012 Sep;135(Pt 9):2581-2. doi: 10.1093/brain/aws228. PMID: 22961541.
31) Alastair Compston, Aids to the Investigation of Peripheral Nerve Injuries. Medical Research Council: Nerve Injuries Research Committee. His Majesty's Stationery Office: 1942; pp. 48 (iii) and 74 figures and 7 diagrams; *with* Aids to the Examination of the Peripheral Nervous System. By Michael O'Brien for the Guarantors of *Brain*. Saunders Elsevier: 2010; pp. [8] 64 and 94 Figures, *Brain*, Volume 133, Issue 10, October 2010, Pages 2838–2844
32) Kooij, H.V., & Helm, F.C. (2005). Observations from unperturbed closed loop systems cannot indicate causality. *The Journal of Physiology, 569*.
33) Ellis CM, Simmons A, Jones DK, et al. Diffusion tensor MRI assesses corticospinal tract damage in ALS. *Neurology* 1999;**53**:1051–1058.
34) Sach M, Winkler G, Glauche V, et al. Diffusion tensor MRI of early upper motor neuron involvement in amyotrophic lateral sclerosis
35) Miscio G, Pisano F, Mora G, Mazzini L. Motor neuron disease: usefulness of transcranial magnetic stimulation in improving the diagnosis. *Clin Neurophysiol* 1999;**110**:975–981.
36) Ravits JM, La Spada AR. ALS motor phenotype heterogeneity, focality, and spread: deconstructing motor neuron degeneration. Neurology. 2009 Sep 8;73(10):805-11. doi: 10.1212/WNL.0b013e3181b6bbbd. PMID: 19738176; PMCID: PMC2739608.

37) Alon Abraham, Vivian E. Drory, Fatigue in motor neuron diseases, Neuromuscular Disorders, Volume 22, Supplement 3, 2012, Pages S198-S202, ISSN 0960-8966, https://doi.org/10.1016/j.nmd.2012.10.013.
38) Kent-Braun, Jane A., and Robert G. Miller. "Central fatigue during isometric exercise in amyotrophic lateral sclerosis." *Muscle & Nerve: Official Journal of the American Association of Electrodiagnostic Medicine* 23.6 (2000): 909-914.
39) Sanjak, M., et al. "Quantitative assessment of motor fatigue in amyotrophic lateral sclerosis." *Journal of the neurological sciences* 191.1-2 (2001): 55-59.
40) Sharma, K. R., et al. "Physiology of fatigue in amyotrophic lateral sclerosis." *Neurology* 45.4 (1995): 733-740.
41) Manschot S, van Passel L, Buskens E, Algra A, van Gijn J. Mayo and NINDS scales for assessment of tendon reflexes: between observer agreement and implications for communication. J Neurol Neurosurg Psychiatry. 1998 Feb;64(2):253-5. doi: 10.1136/jnnp.64.2.253. PMID: 9489542; PMCID: PMC2169960.
42) Marie -Pascale Côté, Gregory A. Azzam, Michel A. Lemay, Victoria Zhukareva, and John D. Houlé. Activity-dependent increase in neurotrophic factors is associated with an enhanced modulation of spinal reflexes after spinal cord injury Journal of Neurotrauma 2011 28:2, 299-309
43) Van den Bos M.A., Higashihara M., Geevasinga N., Menon P., Kiernan M.C., Vucic S. Imbalance of cortical facilitatory and inhibitory circuits underlies hyperexcitability in ALS. *Neurology*. 2018;91:e1669–e1676. doi: 10.1212/WNL.0000000000006438.
44) Vaughan, S.K., Kemp, Z., Hatzipetros, T., Vieira, F. and Valdez, G. (2015), Degeneration of proprioceptive sensory nerve endings in mice harboring amyotrophic lateral sclerosis–causing mutations. J. Comp. Neurol., 523: 2477-2494. https://doi.org/10.1002/cne.23848
45) Raynor EM, Shefner JM. Recurrent inhibition is decreased in patients with amyotrophic lateral sclerosis. Neurology. 1994 Nov;44(11):2148-53. doi: 10.1212/wnl.44.11.2148. PMID: 7969975.
46) Brownstone RM, Lancelin C. Escape from homeostasis: spinal microcircuits and progression of amyotrophic lateral sclerosis. J Neurophysiol. 2018 May 1;119(5):1782-1794. doi: 10.1152/jn.00331.2017.

Appendix A Parameter estimation

As stated above a NMM is used to express the joint dynamics in physiologically relevant parameters. The parameters are estimated by minimizing the following error function in a least square sense[21]:

$$E = \sum_f \sum_i \frac{\hat{\gamma}_{d\theta}{}^2(f)}{1+f} \left| \log\left(\frac{\hat{H}_{T\theta,i(f)}}{H_{T\theta,i(f,p)}}\right) \right|^2 + q \frac{\hat{\gamma}_{da}{}^2(f)}{1+f} \left| log\left(\frac{\hat{H}_{\theta a,i(f)}}{H_{\theta a,i(f,p)}}\right) \right|^2 \quad (5)$$

Where i denotes the task, $\hat{H}$ the estimated FRF of the measurements and H the simulated output of the NMM. The left hand term describes the relative error between the estimated and modeled joint admittance, the right hand term describes the relative error of the reflexive impedance. Factor q was set to 0.125 for all subjects such that both terms in (5) had approximately equal values in the error fit. To emphasize highly linear and low noise behavior, the error function was weighted by frequency and coherence, while emphasizing frequencies within the bandwidth of interest.

Appendix B Internal validation

Sensitivity of the parameter estimation procedure is expressed by the SEM. In order to determine the SEM the covariance matrix P was used[13]. The covariance matrix P was determined from the interdependence of the model parameters on the error space[13]. Which was calculated with the following equation:

$$P = \frac{1}{N} \cdot (J^T \cdot J)^{-1} \cdot E \cdot E^T \quad (6)$$

Where E is the fitting error, N the number of samples of the error function E and J the jacobian matrix. The jacobian matrix is a $N\ x\ Np$ matrix, where Np = 37 the number of estimated parameters, containing the first derivatives of the final error to each parameter. By normalizing the cross-covariance to the auto covariance the interdependence was expressed in percentages. The auto-covariance is given by the diagonal terms of P. Sensitivity of the parameters was given by the standard error of the mean (SEM). The SEM is calculated by taking the square root of the auto-covariance. When the SEM is low compared to the corresponding parameter, the parameter in question has a high sensitivity. High sensitivity indicates that a small change in value has a large contribution on the fitting error.

Appendix C Neuromechanical parameters

From the neuromuscular model the parameters were derived. From these parameters the 20 task dependent parameters are shown for the control and patients groups. The mean of the parameters for the patient and control group are presented in table 4.

Table 4 Neuromechanical parameters

		Control	ALS	P-value
Task	Parameter	Mean (SD)	Mean (SD)	
RT	k	5.50 (2.26)	4.53 (2.72)	0.297
	b	0.10 (0.03)	0.09 (0,04)	0.403
	k_v	0.001 (0.008)	0.003(0.018)	0.742
	k_p	0.18 (0.59)	0.22 (0.67)	0.820
	k_f	0.02 (0.09)	0.03 (0.16)	0.374
$FT_{5\%}$	k	8.73 (3.42)	8.82 (2.34)	0.980
	b	0.08 (0.03)	0.07 (0.03)	0.560
	k_v	-0.07 (0.16)	-0.15 (0.20)	0.374
	k_p	-0.15 (0.90)	-1.49 (0.51)	0.009
	k_f	-0.32 (0.35)	-0.59 (2.60)	0.130
$FT_{10\%}$	k	10.31 (3.16)	10.18 (2.74)	0.915
	b	0.09 (0.04)	0.07 (0.05)	0.387
	k_v	0.006 (0.106)	-0.21 (0.21)	0.003
	k_p	0.05 (2.21)	-1.43 (2.95)	0.172
	k_f	-0.36 (0.21)	-0.74 (0.39)	0.005
PT	k	11.42 (3.29)	10.78 (2.25)	0.588
	b	0.14 (0.06)	0.10 (0.04)	0.082
	k_v	0.001 (0.107)	-0.07 (0.12)	0.159
	k_p	-2.30 (2.49)	-3.67 (4.13)	0.330
	k_f	-0.47 (0.33)	-0.54 (0.40)	0.742